JOURNAL OF PROPULSION AND POWER
Vol. 14, No. 2, March–April 1998

Quasisteady Ablative Magnetoplasmadynamic Thruster Performance with Different Propellants

Giorgio Paccani* and Ugo Chiarotti†
University of Rome "La Sapienza," Rome 00184, Italy
and
William D. Deininger‡
FiatAvio Comprensorio BPD, Colleferro, Rome 00034, Italy

This paper discusses quasisteady, ablative, magnetoplasmadynamic (MPD) thruster operation and performance. Quasisteady MPD thrusters operate with instantaneous power levels of a few megawatts during pulses (shots) that last approximately 1 ms. The MPD thruster used during this study consisted of coaxial electrodes with radially positioned bars of propellant that passed through the sidewall of the anode near the cathode tip. Four different polymer propellants were investigated: 1) polytetrafluoroethylene (Teflon®), 2) ethylene-tetrafluoroethylene resin (Hyflon®), 3) polyethylene, and 4) ethylene-chlorotrifluoroethylene resin (Halar®). Voltage, current, ablated propellant mass, jet velocity, and impulse bit were measured for five different values of energy per shot in the 1666–3000 J range for each propellant. Polyethylene exhibited different electrical behavior (higher discharge voltages and impedances) compared with the other three propellants that showed the typical features of high-ionization regime operation. Polytetrafluoroethylene provided the highest thrust and thrust-to-power ratio figures, whereas ethylene-tetrafluoroethylene resin had the lowest values of these parameters. Polyethylene exhibited the highest exhaust velocity.

Nomenclature

A = oscillation amplitude, m
b = Maecker law coefficient, N A^{-2}
C = capacity, F
E = energy, J
e = electron charge, 1.6×10^{-19} C
F_e = I_b/τ_e, thrust, N
F_w = $\dot{m} \cdot w$, N
f = $F_{em}/\dot{m}$, N s kg^{-1}
I_b = impulse bit, N s
i = current, A
M = mass, molecular/atomic mass, kg
m = ablated mass per shot, kg
$\dot{m}$ = mass flow rate, kg s^{-1}
N_0 = Avogadro number, 6.02×10^{23}
P = power, W
Q, q = charge, C
t = time, s
V = potential, V
v = velocity, m s^{-1}
w = exhaust velocity, m s^{-1}
Z = impedance, Ω
z = level
α_i = ionization degree
η = efficiency
μ_0 = vacuum magnetic permeability, H m^{-1}
ρ = anode-to-cathode radius ratio
τ = discharge duration, s
Ψ = $\int i^2 \, dt$, A^2 s
ω = frequency, s^{-1}

Subscripts
c = critical
d = dissociation
e = equivalent, effective
em = electromagnetic
F = thrust
i = ionization
j = jet
t = thruster
tr = transmission
0 = initial

Received Feb. 28, 1996; revision received July 31, 1997; accepted for publication Oct. 17, 1997.

*Scientist Engineer, Department of Mechanics and Aeronautics, via Eudossiana 18. Member AIAA.
†Engineer, Department of Mechanics and Aeronautics.
‡Senior Scientist, Manager Electric Propulsion, Corso Garibaldi 22. Associate Fellow AIAA.

Introduction

MAGNETOPLASMADYNAMIC (MPD) thrusters produce thrust through the acceleration of ionized propellant species using electromagnetic forces. The propellant, which may initially be in a gas, liquid, or solid state, is ionized directly by the MPD arc. In particular, with solid propellants, the particles available for acceleration are those that the electric arc first ablates from the solid lattice and then ionizes. Hence, in contrast to systems that use liquid or gaseous propellants, the propellant mass-flow rate is not an externally controllable variable. It is determined by the engine geometry, arc, and propellant characteristics, and by the arc–propellant interaction.[1] Therefore, thruster behavior is determined by the physical/chemical propellant properties that influence the ablation process.

In the past, studies on ablative thrusters, known as pulsed plasma thrusters (PPTs), were carried out with different propellants.[2,3] PPTs produce thrust over current pulses of several microseconds with energies per shot of tens of joules. In comparison, quasisteady, ablative MPD thrusters are characterized by a current pulse with a square profile (see Fig. 1) that has a much longer duration (more than 1 ms) and a much higher energy per shot (thousands of joules). Here, the current exhibits a plateau with a constant current phase. This paper discusses a comparative experimental analysis of an ablative, coaxial MPD thruster operating on four different propellants.

Propellant Selection

A low ionization potential is the main criterion for propellant selection[4] because low ionization potentials minimize energy

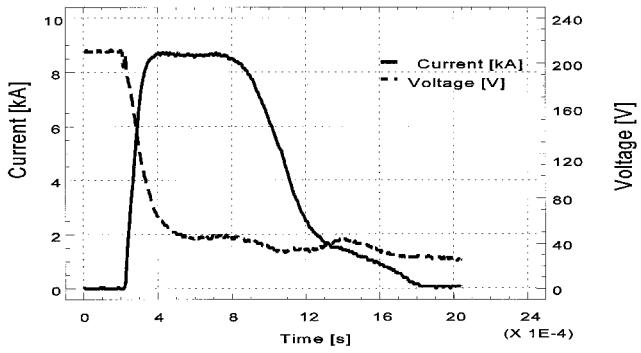

Fig. 1 Typical quasisteady, ablative MPD discharge current–voltage characteristic.

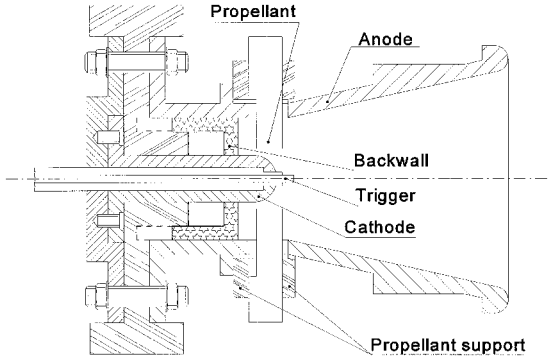

Fig. 2 Schematic of the coaxial, ablative MPD thruster.

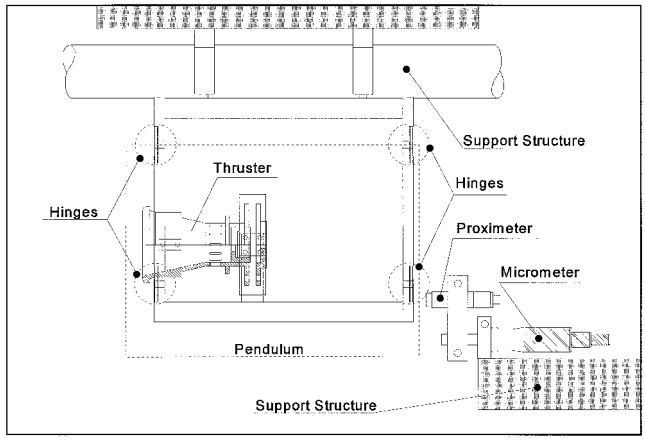

Fig. 3 Thruster accommodation in the thrust stand.

losses. In the past, propellants consisting of a substrate seeded with substances of low ionization potential were used,[5] most notably polymers impregnated with alkaline and alkaline-Earth metals. No substantial progress was made in improving engine performance using this solution.[2]

Alternate materials selection criteria include low vaporization and dissociation energies and/or low sublimation temperatures. Therefore, some iodine-based compounds and plastic materials can be considered as propellants.

Furthermore, solid propellants that contain elements that strongly react with their own surface once transformed into gas can provide performance advantages. Hence, fluoropolymers should provide advantages[6] because they release fluorine, an extremely reactive substance.

In addition, the propellant should be an electrically insulating material so that the arc energy is used for ablation and not simply carried away by unbound electrons in the solid lattice. However, some insulating substances may promote the formation of a conductive surface coating that could inhibit the ablation process.[2,7] Furthermore, if the thruster design provides for propellant contact with both electrodes, any conductive coating could create a short between the electrodes and reduce the energy available for the discharge.

The characteristics of plastic polymers make them most suitable to serve as propellants for MPD thrusters. They are easily sublimated over a wide range of temperatures and pressures. They possess good mechanical properties and high electrical resistivity. Furthermore, the gas generated by their sublimation can be easily ionized. These polymers have provided the best performance when utilized as the propellant in PPTs, particularly polytetrafluoroethylene.[2]

As a result of the preceding considerations, the following four materials were chosen as propellants for this experimental analysis: 1) polytetrafluoroethylene (PTFE) [$(C_2F_4)_n$, Teflon®]; 2) ethylene-tetrafluoroethylene resin (ETFE) [$(C_2H_4-C_2F_4)_n$, Hyflon®, Tefzel®]; 3) polyethylene (PE) [$(C_2H_4)_n$]; and 4) ethylene-chlorotrifluoroethylene resin (ECTFE) [$(ClC_2F_3-C_2H_4)_n$, Halar®].

Experimental Details

The thruster and facility used during the tests described in this paper are summarized next. The test measurements and procedures are also summarized.

Thruster System

The thruster system used in the experiments was composed of a pulse-forming network (PFN) with a total capacity of 0.072 ± 0.002 F split into two 15-capacitor branches tied to a coaxial MPD thruster. The PFN set voltage was the controllable parameter during the tests.

The coaxial MPD thruster (Fig. 2) had a divergent anode made from aluminum with an inlet diameter of 47 mm, a half-angle of 12.5 deg, and an area ratio of 3:1. The tungsten cathode diameter was 18 mm. A total of six propellant bars passed through the anode wall and symmetrically surrounded the cathode tip. The cross section of each propellant bar measured 11 by 3 mm. The discharge was triggered with a 0- to 20-kV power supply connected to a 2-mm-in diam tungsten rod that served as the trigger. The trigger electrode was imbedded along the centerline of the MPD cathode and protruded from the cathode tip (Fig. 2). The trigger electrode and cathode were isolated from each other by an insulating sleeve. During the experiments the trigger was always set below 10 kV. The thruster was mounted on the thrust balance using four insulating support bars.

Facility

The tests described here were conducted in a 0.5-m^3, polyvinyl chloride (PVC), vacuum tank with a backpressure of $(7.5 \pm 2.5) \times 10^{-3}$ Pa. All of the instrumentation was housed in a full Faraday cage. Data acquisition of all measurements was fully computer controlled.

A thrust balance, shown schematically in Fig. 3, was used to measure the thruster impulse bit and evaluate engine performance. It is described in detail in Ref. 8. Briefly, a thruster shot causes the thrust-balance-suspended pendulum to oscillate as illustrated in Fig. 4. An analysis of this oscillation has shown that the impulse bit is given by[8]

$$I_b = M_e A \omega \tag{1}$$

where M_e is the equivalent pendulum mass, A is the oscillation amplitude (Fig. 4), and ω is its natural frequency. The instantaneous position of the pendulum was measured using a 0.001-mm-resolution proximeter.

Test Measurements and Procedures

The following quantities were measured during each shot: the instantaneous values of the electrical parameters [anode-

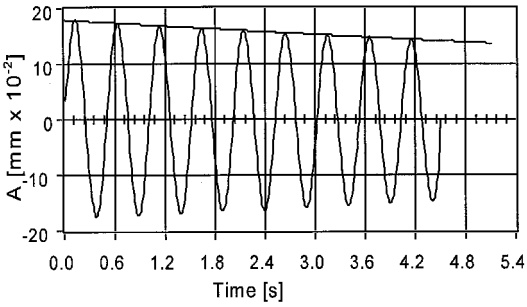

Fig. 4 Computerized elaboration of the thrust stand pendulum motion.

to-cathode potential difference $V(t)$ and discharge current intensity $i(t)$], the ablated mass per shot, m, the impulse bit, I_b, and the jet exhaust velocity w.

The electrode potential was measured directly using an oscilloscope while the current was measured using a Rogowsky probe. A value averaged over 30 measurements was used as the standard value for each electrical parameter.

The energy per shot E_t

$$E_t = \int_0^\infty i(t) \cdot V(t)\, dt \tag{2}$$

and the total transferred charge Q

$$Q = \int_0^\infty i(t)\, dt \tag{3}$$

were computed using the measured electrical parameters through Eqs. (2) and (3).

The ablated propellant mass was obtained by weighing the propellant bars before and after each series of shots using an electronic balance with an accuracy of ± 1 mg. The error in this measurement has been estimated to be a maximum of ± 5 mg because of propellant handling and trigger insulator material deposition. The number of shots in each series was chosen so that the ablated mass exceeded 50 mg.

The impulse bit value was taken as an average of five measurements derived from the thrust stand data as described earlier.[8]

Finally, the exhaust velocity was taken as the average value from 30 time-of-flight measurements of thruster shots at the same conditions based on the cross correlation of the signals from two double langmuir probes located downstream of the thruster.[9] This method permitted measurement of the ion velocity.

Each measurement was taken for different levels of PFN stored energy E_0

$$E_0 = \tfrac{1}{2} C V_0^2 \tag{4}$$

which were obtained by setting the initial voltage value, V_0. The measurements were made for E_0 in the 1660- to 3000-J range using energy steps of $\sim$330 J.

To compare shots with different current–time histories the parameter Ψ is used:

$$\Psi = \int_0^\infty i^2(t)\, dt \tag{5}$$

Moreover, to compare quasisteady operation with steady-state operation, quantities averaged over the discharge duration have to be considered. The quasisteady discharge is characterized by a long tail with an extremely low current value (Fig. 1), which has a negligible contribution to thruster performance. Therefore, the discharge duration is assumed to be the conventional time interval τ_e defined by the expression

$$\int_0^{\tau_e} i^2(t)\, dt = 0.98\Psi \tag{6}$$

Using Ψ and τ_e, it is possible to define an effective current

$$i_e = (\Psi/\tau_e)^{1/2} \tag{7}$$

an effective impedance

$$Z_e = E_t/\Psi \tag{8}$$

and an effective voltage

$$V_e = Z_e \cdot i_e \tag{9}$$

Moreover, an equivalent thrust can also be defined

$$F_e = I_b/\tau_e \tag{10}$$

and similarly other propulsive parameters.

To compare engine performance on the various propellants, the values of their average molecular weight and ionization energy were computed. The average ionization energy was assumed to be the sum of the ionization energies of the single dissociated elements[10] (see Table 1).

Because each data point represents many thruster shots, errors were calculated using error propagation theory based on the standard deviation of the individual measurements.

Experimental Results and Discussion

General Remarks

The thruster exhibited normal operation over the whole energy range with all propellants except PE. Operation with PE was often irregular, particularly at lower energies, and exhibited much broader standard deviation values (in particular in the exhaust velocity measurements). The high level of irregularity prevented reproducible results at the lowest energy level.

Electrical Parameters

The characteristic $V_e - i_e$ curve increases linearly as shown in Fig. 5 (increasing shot energy E_0), whereas the impedance exhibits a decreasing trend that tends asymptotically to a constant value[1] as shown in Fig. 6. The asymptotic limit is approximately 8 mΩ, whereas ETFE exhibits higher discharge voltages and impedances. The arc voltage values vary from 75 to 95 V, whereas the impedance values range between 8.5 and 12 mΩ.

The efficiency of the conversion of stored electrical energy to discharge energy is given by

$$\eta_{tr} = E_t/E_0 \tag{11}$$

which decreased slightly with energy because the arc impedance dropped asymptotically but was always between 0.45 and 0.50.

The parameter Ψ shows the typical linear trend with increasing energy. The $\Psi - E_0$ curves for each propellant lie along the same characteristic line except for the curve relative to ETFE, which is slightly lower (Fig. 7).

During the tests with ECTFE, some of the propellant bars were installed incorrectly. These bars were in contact with both electrodes and a partially electrically conductive coating formed. This coating allowed a current to pass between the electrodes and the discharge started spontaneously when the po-

Table 1 Molecular weights and averaged ionization energies for each propellant

Propellant	$(C_2F_4)_n$	$(C_2H_4 - C_2F_4)_n$	$(C_2H_4)_n$	$(ClC_2F_3 - C_2H_4)_n$
M, g/mole	16.67	10.67	4.67	12.08
ε_a, eV/atom	15.77	14.28	12.79	13.86

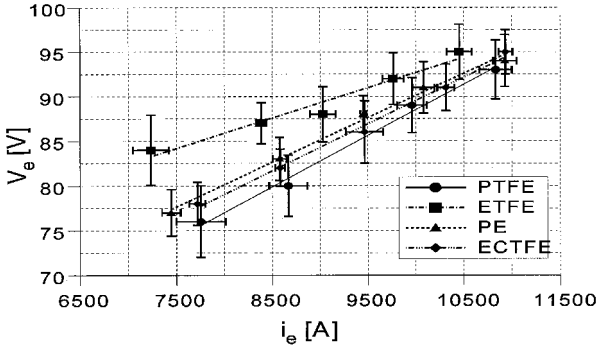

Fig. 5 Ablative MPD voltage–current characteristics for different propellants.

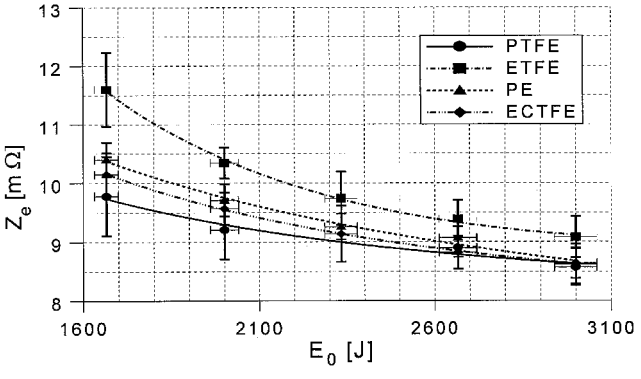

Fig. 6 Ablative MPD impedance vs stored energy E_0 characteristics for different propellants.

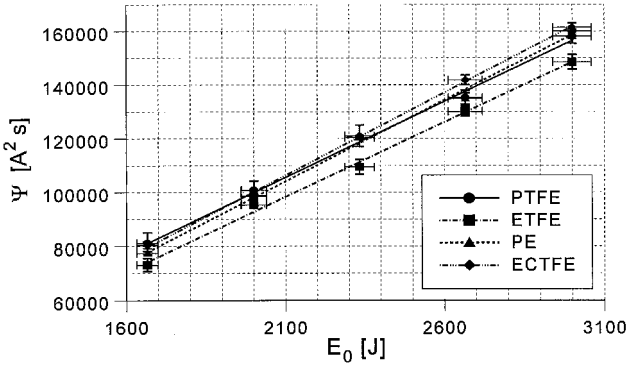

Fig. 7 Ablative MPD Ψ parameter vs stored energy E_0 characteristics for different propellants.

tential difference reached approximately 100 V. This phenomena is believed to be caused by the sublimation of the coating and a surface layer of propellant through joule heating of the coating. In other words, the coating was vaporized and acted as a low voltage trigger contrary to expectations.[2,7]

The discharge duration τ_e [Eq. (6)] was found to be constant with energy and similar for all propellants with a value of $\tau_e \approx 1.35 \pm 0.013$ ms.

Ablated Mass

The ablated mass m was found to increase linearly with energy E_t and, through Eq. (8), with the parameter Ψ (Fig. 8).

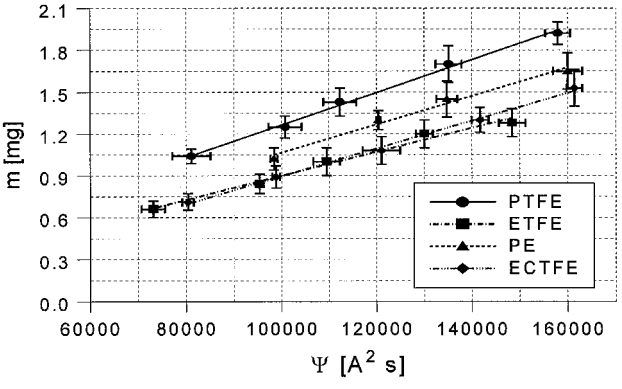

Fig. 8 Ablated propellant mass vs the Ψ parameter.

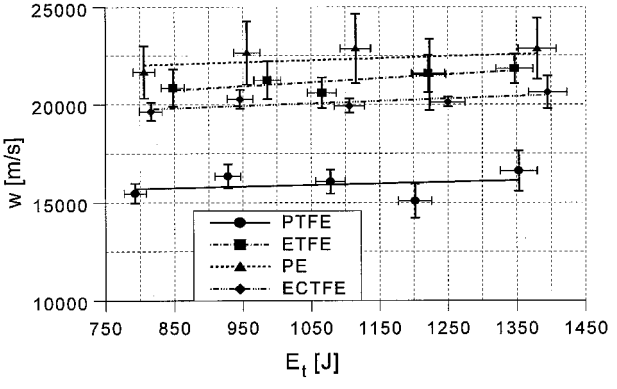

Fig. 9 Ablative MPD exhaust velocity as a function of the energy E_t for different propellants.

If energy or Ψ is held constant, the following relationship is valid:

$$m(\text{PTFE}) > m(\text{PE}) > m(\text{ECTFE}) \geq m(\text{ETFE}) \qquad (12)$$

Exhaust Velocity

The exhaust velocity was found to increase slightly with increasing energy for all propellants (Fig. 9), as shown in previous studies.[1] Furthermore, assuming constant E_t, the following relation among the exhaust velocities was shown to be valid:

$$w(\text{PE}) > w(\text{ETFE}) > w(\text{ECTFE}) > w(\text{PTFE}) \qquad (13)$$

The propellants with lower molecular weights had higher velocity values. ETFE, ECTFE, and PTFE exhibited the same basic relationship between velocity and molecular weight at equal energy. However, the measured velocity for PE was much lower (Fig. 9), than expected from the velocity–molecular weight relationship.

The measured velocity is biased by the degree of ionization due to the measurement technique. Generally speaking, this parameter is difficult to compute. However, assuming the same average ionization level for all existing species ($z_i = q_i/e = \text{const}$), a rough indicator α_i may be identified for comparison purposes only. This indicator is based on the computable quantities transferred charge Q and ablated mass m per shot

$$\alpha_i = \frac{Q}{q_i N} = \frac{QM}{q_i z_d m N_0} \qquad (14)$$

where N is the number of ablated particles. Because charge varies with current and mass varies with the current squared (Fig. 8), it follows that the charge-to-mass ratio Q/m varies inversely with current. Therefore, on the basis of this expression, full ionization may be inferred for PTFE, ETFE, and ECTFE while a half-ionization condition (or less) appears to be present for PE.

This may explain why the ion velocity measured for PE is much lower than what would be expected on the basis of the molecular weight alone. Ions can be slowed down through collisions with slow-moving neutrals through both energy exchange and charge exchange mechanisms.

Some phenomena taking place in MPD thrusters have been correlated[11,12] to the Alfvén velocity[13]

$$v_c = \left(\frac{2eV_i}{M}\right)^{1/2} \tag{15}$$

and to the critical ionization current, corresponding to the full ionization regime[14]

$$i_{ec}^2 = \frac{\dot{m}}{b} v_c = \frac{\dot{m}}{b}\left(\frac{2eV_i}{M}\right)^{1/2} \tag{16}$$

These quantities have a strict physical meaning if calculated for single-component propellants such as gaseous argon-fed thrusters. Here these parameters must be calculated as average values in a fully dissociated, multicomponent propellant and are given in Table 2. The first three propellants show mean exhaust velocities higher than the respective Alfvén velocities v_c, whereas PE shows a velocity very close to the respective Alfvén velocity. These results agree with the Block–Fahleson experiment.[13]

In general, equal MPD thrusters operating with the same current but with different propellants will have different propellant mass-flow rates or, for solid propellant thrusters, different propellant consumption rates. Therefore, to compare thruster operation on different propellants, the specific thrust (Fig. 10) must be considered

$$f = F_{em}/\dot{m} = b(i_e^2/\dot{m}) = bi_e^{*2} \tag{17}$$

Table 2 Measured ion velocities compared to the calculated Alfvén velocities

Propellant	PTFE	ETFE	PE	ECTFE
$\bar{w}$, m/s	15,900	21,200	22,300	20,200
v_c, m/s	13,500	16,100	23,000	14,900

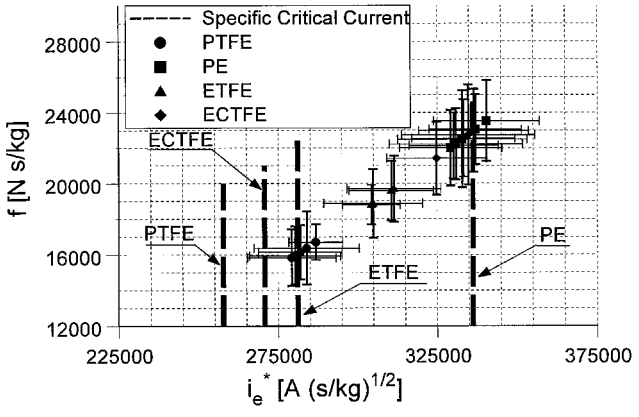

Fig. 10 Ablative MPD specific thrust vs specific current for different propellants.

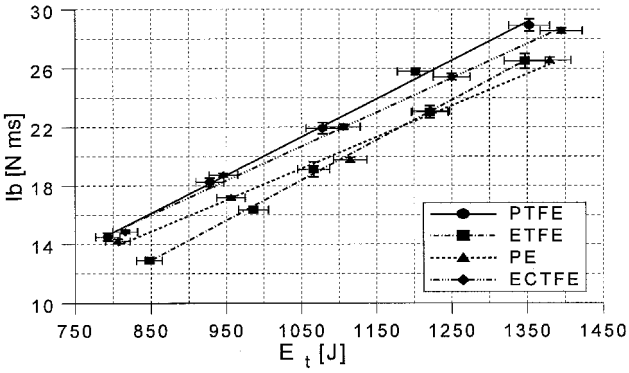

Fig. 11 Ablative MPD impulse bit vs energy E_t for different propellants.

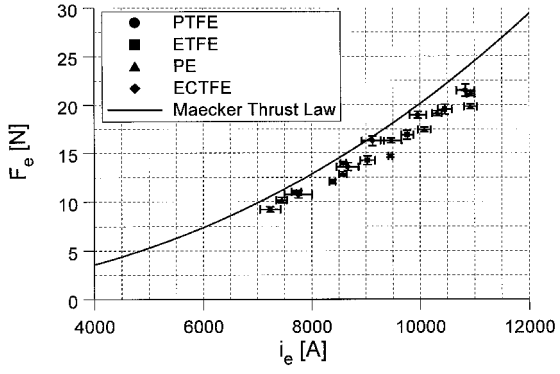

Fig. 12 Ablative MPD thrust vs current for different propellants with the Maecker thrust law.

where a specific current has been introduced:

$$i_e^{*2} = i_e^2/\dot{m} = \Psi/m \tag{18}$$

These test results coupled to previous results,[1] which included different solid propellant configurations, different engine geometries, etc. (also see Fig. 8) demonstrate conclusively that this is a constant characteristic of each propellant. A specific critical ionization current can also be introduced:

$$i_{ec}^{*2} = \frac{i_{ec}^2}{\dot{m}} = \frac{1}{b} v_c = \frac{1}{b}\left(\frac{2eV_i}{M}\right)^{1/2} \tag{19}$$

The experimentally measured specific current values (Fig. 10) are all larger than the specific critical ionization current values calculated using Eq. (19) except for PE, which shows lower values.

Impulse Bit and Thrust

During the discharge, the operation of a quasisteady MPD thruster may be compared with steady-state operation through the use of the effective current i_e [Eq. (7)]. Because the discharge time interval τ_e [Eq. (6)] is basically the same for each propellent, all considerations regarding the measured impulse bit also apply to the thrust ($F_e = I_b/\tau_e$). The impulse bit increases with increasing discharge energy E_t as shown in Fig. 11. The slope of the curve for PE is smaller than for the other propellants. The following relationship was defined based on the experimental measurements:

$$I_b(\text{PTFE}) > I_b(\text{ECTFE}) > I_b(\text{PE}) \geq I_b(\text{ETFE}) \tag{20}$$

Thrust follows the Maecker law[15] as shown in Fig. 12

$$F_{em} = bi^2 \tag{21}$$

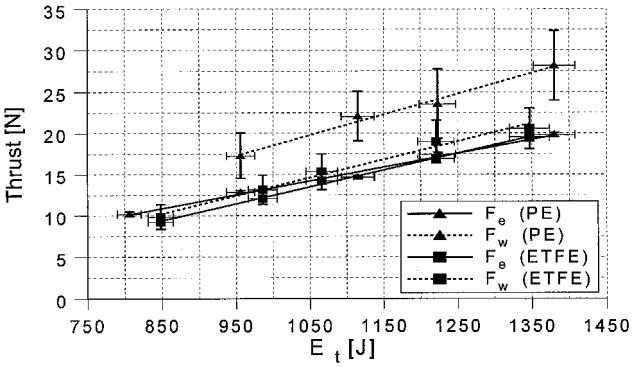

Fig. 13 Ablative MPD thrust vs energy E_t for different propellants.

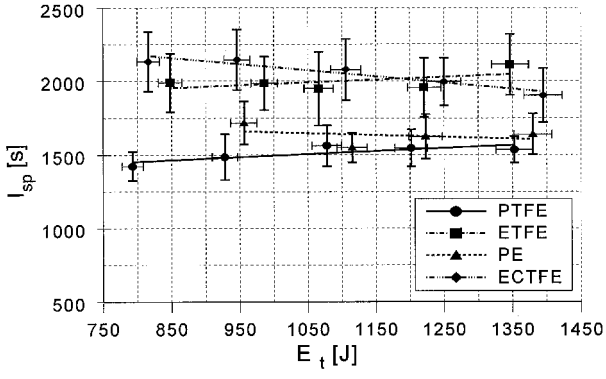

Fig. 14 Ablative MPD specific impulse vs energy E_t for different propellants.

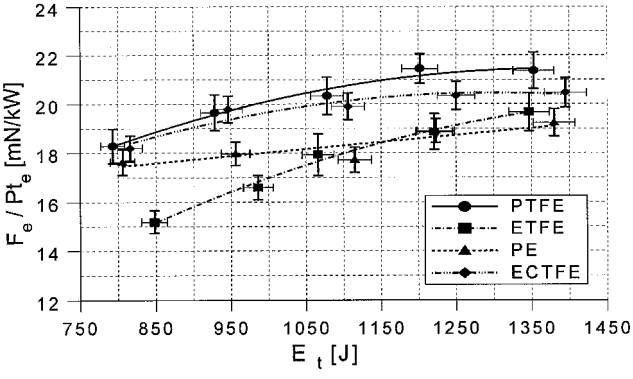

Fig. 15 Ablative MPD thrust-to-power ratio vs energy E_t for different propellants.

where

$$b = (\mu_0/4\pi)(\ell n\, \rho + \tfrac{3}{4}) \tag{22}$$

Here, ρ is the anode-to-cathode radius ratio. Because the anode was conically shaped, the average value of the cone radius was used as the anode radius. The Maecker law predicts higher values than measured experimentally. This might depend on the calculated value of the b parameter. Notice that, in calculating b, the anode radius physically represents the average radius of the axial current distribution along the anode. Its value is smaller than the value assumed here because the discharge tends to concentrate on the initial tract[16] where the anode radius is smaller.

Computation of the thrust F_w, as mass-consumption rate times exhaust velocity, provides similar or higher values than those measured experimentally, F_e as shown in Fig. 13, although the slopes are very similar and the experimental uncertainties are fairly large. The gap between calculated and experimental values is small for all the propellants except PE. This is consistent with the previous calculation of the ionization degree [Eq. 14)] and the discussion on the velocity of PE. Because the measured ion velocity is much higher than the velocity of the neutral species, the gap between F_w and F_e is higher when the ionization degree is lower. This can be seen by considering the specific impulse (Fig. 14). The specific impulse values for PE were found to be smaller than for the other propellants, whereas the measured exhaust velocities (Fig. 9) were always higher.

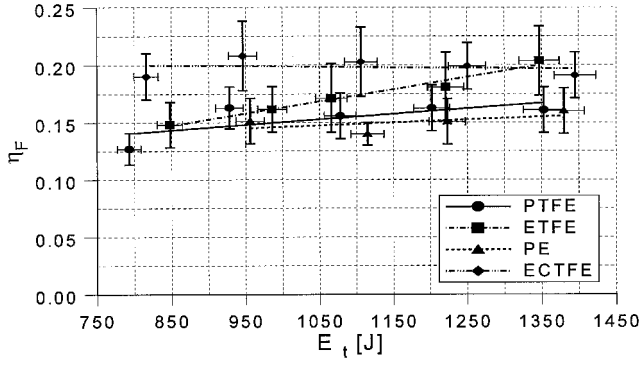

Fig. 16 Ablative MPD thrust efficiency vs energy E_t for different propellants.

The thrust-to-power ratio ($F_e/P_{te} = I_b/E_t$) increases with E_t (Fig. 15) and tends toward a constant value for each propellant. PTFE exhibits the highest thrust values over the input energy range tested while the ETFE characteristic has the steepest slope.

Thrust Efficiency

Finally, thrust efficiency, given by the following equation exhibits a slightly increasing trend with the shot energy for all propellants except for ETFE, which has a much steeper slope (Fig. 16):

$$\eta_F = \frac{E_j}{E_t} = \frac{I_b^2}{2mE_t} \tag{23}$$

At the higher energy levels, the relationship between the propellants is

$$\eta_F(\text{ECTFE}) \approx \eta_F(\text{ETFE}) \geq \eta_F(\text{PTFE}) > \eta_F(\text{PE}) \tag{24}$$

Conclusions

This paper discussed the operation and performance of a quasisteady, ablative, MPD thruster with four different polymer propellants. The MPD thruster consisted of coaxial electrodes with radially positioned bars of propellant that passed through the sidewall of the anode near the cathode tip. PTFE, ETFE, PE, and ECTFE propellants were investigated. Voltage, current, ablated propellant mass, jet velocity, and impulse bit were measured for five different values of energy per shot in the 1666–3000 J range for each propellant. Teflon, Hyflon, and Halar exhibited similar behavior and showed typical features of a high-ionization regime operation. Polyethylene exhibited different electrical behavior (higher discharge voltages and impedances) compared with the other three propellants and appeared to operate in a partially ionized regime. As shown in previous studies[1] with ablative MPDs of diverse geometries, as the shot energy increases, the electrical behavior tends to stabilize because the impedance goes toward a minimum value asymptotically while there is a linear dependance between the shot energy and thrust, and the ratio between thrust and energy tends toward a constant dependent on the propellant and geometry. Furthermore, the thrust characteristic was generally similar for all four propellants, and the Maecker thrust law was

shown to be valid for the operational envelop of this study. The highest thrust and thrust-to-power ratio figures were provided by Teflon, whereas Hyflon had the lowest values of these parameters. Polyethylene exhibited the highest exhaust velocity. Higher thrust efficiencies were seen for Halar and Hyflon.

Acknowledgments

This work was sponsored by the Ministry of University Research in Science and Technology through Grant 1994, and by the Italian Space Agency through Contract 92-RS-27. The authors thank the reviewers and associate editor for their positive and constructive approach to reviewing this manuscript.

References

[1]Paccani, G., "Non-Steady Solid Propellant MPD Thruster Experimental Analysis Concepts," AIAA Paper 90-2674, July 1990.

[2]Palumbo, D. J., and Guman, W. J., "Pulsed Plasma Propulsion Technology," Air Force Rocket Propulsion Lab., TR-73-79, Sept. 1973.

[3]Leiweke, R. J., Turchi, P. J., Kamhawi, H., and Myers, R. M., "Experiments with Multi-Material Propellants in Ablation-Fed Pulsed Plasma Thrusters," AIAA Paper 95-2916, July 1995.

[4]Paccani, G., and Chiarotti, U., "Behaviour of Quasi-Steady Ablative MPD Thrusters Performance with Different Propellants," International Electric Propulsion Conf., Paper 95-118, Sept. 1995.

[5]Polk, J. E., and Pivirotto, T. J., "Alkali Metal Propellant for MPD Thrusters," AIAA Paper 91-3572, Sept. 1991.

[6]Myers, R. M., "Electromagnetic Propulsion for Spacecraft," AIAA Paper 93-1086, Feb. 1993.

[7]Liebing, L., and Seidel, F., "A Low Current Pulsed Ablation Plasma Thruster," AIAA Paper 73-1068, Oct. 1973.

[8]Paccani, G., and Ravignani, R., "Sistemi di Misura della Spinta di Propulsori MPD," *Aerotecnica Missili e Spazio*, Vol. 72, No. 1, 1994, pp. 42–51 (in Italian).

[9]Paccani, G., and Di Zenzo, S., "MPD Thrusters Computer Operated Jet Velocity Measurement," *Aerotecnica Missili e Spazio*, Vol. 74, No. 3-4, 1995, pp. 93–102.

[10]Paccani, G., and Chiarotti, U., "Propellenti," *Studi sui Meccanismi Fisici di Base nei Propulsori MPD*, Italian Space Agency, Rept. III, Jan. 1996 (in Italian).

[11]Choueiri, E. Y., Kelly, A. J., and Jahn, R. G., "The Manifestation of Alfvén's Hypothesis of Critical Ionization Velocity in the Performance of MPD Thrusters," AIAA Paper 85-2037, Sept. 1985.

[12]Turchi, P. J., "Critical Speed and Voltage-Current Characteristics in Self-Field Plasma Thrusters," *Journal Propulsion and Power*, Vol. 2, No. 5, 1986, pp. 398–401.

[13]Alfvén, H., "Collision Between a Non-Ionized Gas and a Magnetized Plasma," *Reviews of Modern Physics*, Vol. 32, No. 4, 1960, pp. 710–713.

[14]Choueiri, E. Y., "An Introduction to the Plasma Physics of the MPD Thruster," Dept. of Mechanical and Aerospace Engineering, Princeton Univ., Progress Rept. 1776.34, Princeton, NJ, Nov. 1991.

[15]Maecker, H., "Plasmaströmungen in Lichtbögen infolge eigenmagnetischer Kompression," *Zeitschrift für Physik*, Bd. 141, 1955, pp. 198–216 (in German).

[16]Paccani, G., "Experimental Analysis of a Coaxial Solid Propellant MPD Thruster with Segmented Anodes," International Electric Propulsion Conf., Paper 93-159, Sept. 1993.